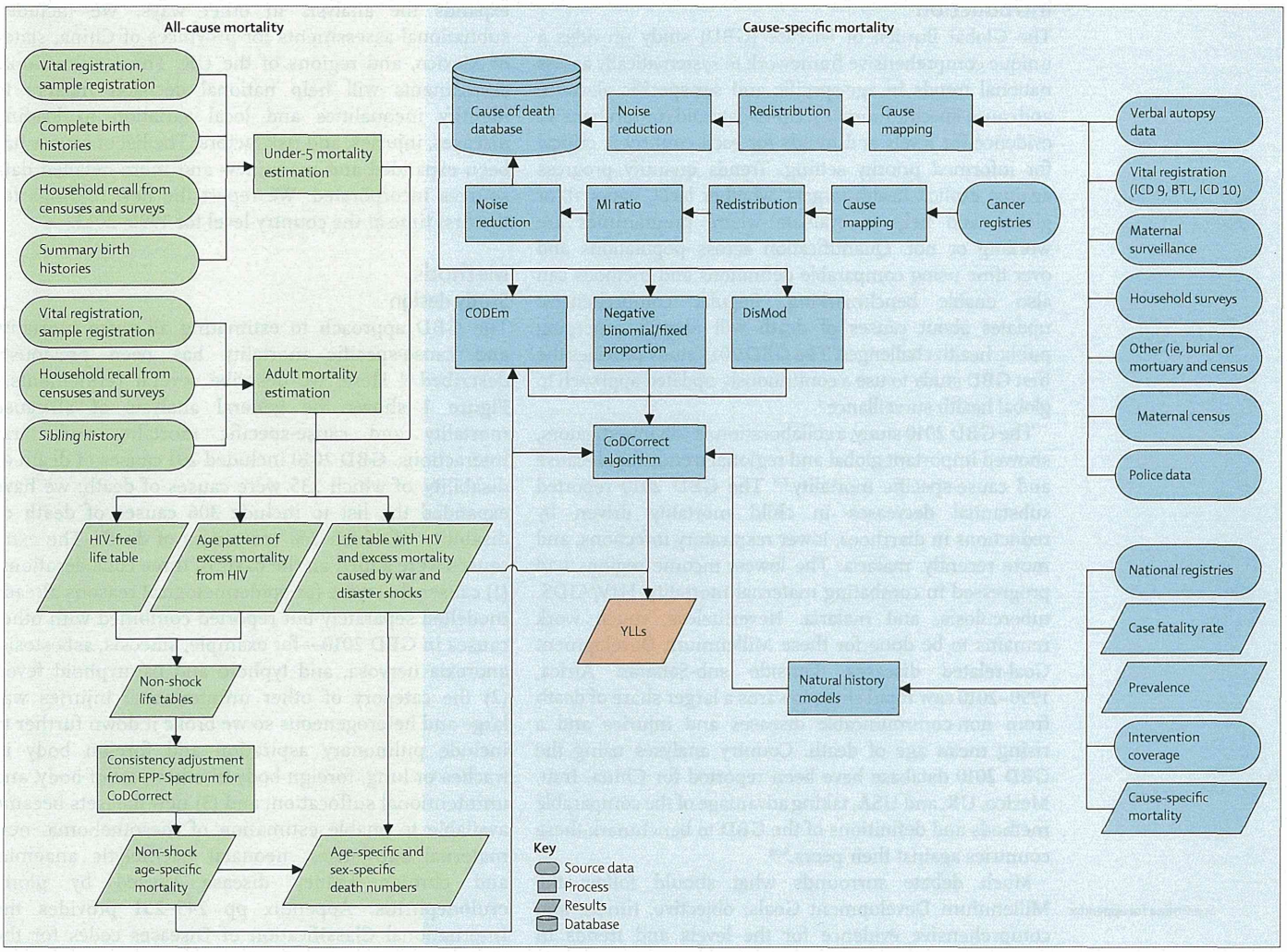

Figure 1: **Components of GBD 2013 and their relations**
ICD=International Classification of Diseases. BTL=basic tabulation list. MI ratio=mortality:incidence ratio. CODEm=Cause of Death Ensemble model. YLLs=years of life lost. EPP=UNAIDS Estimates and Projects Package.

Covariates

We estimated national time series (1980–2013) for a range of covariates with data from surveys (household-level and individual-level data), censuses, official reports, administrative data, and a systematic review. For lagged distributed income and education, we estimated national time series from 1950, to 2013. Details of how we imputed series for GDP, educational attainment, tobacco prevalence, and obesity prevalence have been published previously.[29–32] Appendix (pp 4961–4974) shows the sources and imputation methods used to generate time series for each covariate. Generally, we estimated uncertainty in covariate values when sufficient information was available.

All-cause mortality

We analysed all-cause mortality for 188 countries from 1950 to 2013; we present only results for 1990–2013 to coincide with the period of the overall GBD 2013 assessment. As a result of the split of Sudan, we re-extracted data and made new separately generated estimates for Sudan and South Sudan. We improved how we adjusted for data source bias for the analysis of child mortality in two ways. First, by using the improved functional forms between summary mortality indicators for child (age <5 years) and adult (age 15–59 years) age groups and other covariates, including crude rates of death caused by HIV/AIDS. And second, by modification of the model lifetable system to use a unified standard life-table selection process and improved re-distribution of excess mortality rate from HIV/AIDS. We divided the analysis into eight steps. Input data and key indicators for all countries are available online.

First, to estimate under-5 mortality ($_5q_0$), we analysed all survey, census, sample registration, and vital registration sources. Wherever possible, we analysed microdata from surveys and censuses with updated methods for child mortality.[33] We synthesised all measurements of under-5

For the **input data and key indicators for each country** see http://vizhub.healthdata.org/mortality/

mortality with spatiotemporal regression and Gaussian process regression.[33] We corrected for bias in different sources in specific countries.

Second, to estimate adult mortality ($_{45}q_{15}$), we systematically identified all available vital registration data, sibling history survey data, sample registration data, and household recall of deaths. We assessed vital registration data for completeness by optimised death distribution methods.[2,34] We analysed sibling history data to account for survivor bias, zero-surviving sibships, and recall bias.[2,35] We synthesised sources with a combination of spatiotemporal regression and Gaussian process regression. The mean function for the Gaussian process regression was based on the combination of a non-linear hierarchical model with income per person, mean years of education in age group 15–60 years, mortality caused by HIV/AIDS, and country random effects[2] as covariates, and a spatiotemporal regression in which we added to the first stage model without country random effects, the smoothed residuals between the first stage model and observed data (appendix pp 66–79). We selected the hyper-parameters for Gaussian process regression through an out-of-sample predictive validity testing process.[2] We ranked the estimated subnational adult mortality in China, India, Mexico, and the UK to ensure that the sum of subnational estimates for a given age-sex group equalled the national estimates accounting for different population sizes.

Third, we assessed HIV-free under-5 mortality and adult mortality. HIV/AIDS causes more excess mortality in younger people and thus changes the age pattern of mortality that otherwise can be readily described by Gompertz law of mortality or the Kannisto-Thatcher model.[36,37] Where HIV/AIDS is common, this pattern of mortality should be explicitly taken into account. We estimated the HIV-counterfactual under-5 mortality and adult mortality rates using the estimated coefficients of crude death rate from HIV from the non-linear mixed effects models for under-5 mortality and adult mortality respectively, and setting the crude death rates from HIV/AIDS in the respective age groups to zero (appendix pp 90–94).

Fourth, we constructed an HIV-free life-table. The GBD 2010 introduced a model life-table system that used the under-5 death rate and adult mortality rate along with a selected standard mortality schedule to estimate the full age pattern of mortality for country-years of interest.[33] For GBD 2013, we modified how the standard mortality schedule was selected for each country-year so that the same approach was used for all countries. Specifically, we empirically computed a set of space-time weights that relate the observed age pattern of the probability of death in a sex-country-year with other sex-country-year observations. These weights were derived by comparing every empirical life-table that is not affected by the HIV/AIDS epidemic in the GBD database (10 673 life-tables) with every other life-table for the same sex. We estimated space-time weights as a function of the time lag between the paired life-tables and location (ie, within the country, region, or super-region). We estimated these weights as the inverse of the average sum of age-specific differences in the logit of the probability of death (appendix pp 79–91). The key observation from this spatial-temporal analysis of age-specific probabilities of death is that the mortality pattern in a country in a given year was more strongly related to the mortality pattern in the same country within 15 years than to mortality patterns in other countries; however, other countries in the same region or other regions generally are similarly related when the lag-in time was more than 20 years.

Fifth, we assessed the age pattern of HIV/AIDS mortality. Excess mortality from HIV/AIDS as quantified between the estimated $_5q_0$ and $_{45}q_{15}$ with their HIV counterfactual counterparts leads to increased mortality in specific age groups. This excess HIV/AIDS mortality was assigned by age with the estimated relative risk of death caused by HIV/AIDS in an age group compared with the HIV/AIDS excess death rate in age group 40–44 years. We estimated these relative risks with data from vital registration systems that have International Classification of Diseases 10 coded causes of death from HIV/AIDS, which includes South Africa.[38] We used Seemingly Unrelated Regression model[39] with only a constant and generated 95% uncertainty intervals (UIs) for the age pattern of relative risks by repeatedly sampling from the mean and covariance matrix of the estimated βs and the error term. Seemingly Unrelated Regression enables the error term of a series of linear regressions to be correlated. We used separate regressions by sex and for the pattern of mortality in concentrated epidemics and generalised epidemics as defined by UNAIDS.[38–40]

Sixth, we minimised the difference between demographic estimation of age-specific mortality and HIV models. Murray and colleagues[38] used a refined version of the EPP-Spectrum framework to model HIV/AIDS mortality. This analysis yielded very large UIs for HIV/AIDS in many countries. However, in some southern African countries, there remained a large discrepancy between data for all-cause mortality and estimates of HIV/AIDS mortality with demographic sources suggesting smaller epidemics. To minimise the difference between HIV/AIDS mortality and the demographic estimates, which are also uncertain, we computed a loss function that quantifies the extent to which the age-sex-country-year HIV/AIDS estimates exceed all-cause mortality:

$$e_r = \sum_t \sum_a \sum_s \max(0, m^{HIV}_{r,t,a,s} - 0{\cdot}8 \times m^{all\text{-}cause}_{r,t,a,s})$$

For run (r) of a given country, excess mortality (e) is equal to the sum of all non-zero differences between HIV/AIDS mortality (m^{HIV}) and 0·8 times a randomly selected all-cause mortality draw ($m^{all\text{-}cause}$) across all year

(t), age (a), and sex (s) combinations. 0·8 was the highest observed cause fraction caused by HIV in any age group in any vital registration system. We selected from the uncertainty ranges for HIV and all-cause mortality those that minimised the difference. If no draws had a positive loss function, we sampled randomly from all matched draws.

The CoDCorrect algorithm includes HIV/AIDS cause-specific mortality and can alter the age and time distribution of deaths from HIV/AIDS. To incorporate the overall change in the number of HIV/AIDS deaths over the course of the epidemic in a country implied by the application of the CoDCorrect algorithm, but not to distort the Spectrum estimated time and age pattern, we adjusted the entire HIV/AIDS epidemic up or down on the basis of the cumulative effects of CoDCorrect on HIV/AIDS for all estimated years in each country.

Seventh, we used the same method as Wang and colleagues[2] to generate child mortality rate and adult mortality rate for natural disasters and armed conflicts. We obtained data for conflict and war, including deaths from one-sided violence, non-state conflict, armed force battles, and other national or international conflicts, from the Uppsala Conflict Data Program[41] and the International Institute for Strategic Studies.[42] Further data for war were obtained from countries' vital registration systems and classified as caused by war.[43] We included disaster data from the International Disaster Database from the Center for Research on the Epidemiology of Disasters (University of Louvain, Brussels, Belgium).[44] From this database, we included deaths caused by complex disaster, drought, earthquake, flood, and others. When these databases were not fully up-to-date or did not contain shocks known to exist, we supplemented with case-by-case sources. These with-shock mortality rates were then used as entry parameters to the GBD relational model life-table system to generate age-specific mortality rates with the effect of shocks added.

Eighth, we used age-specific and sex-specific death rates from the life-table to generate numbers of death by multiplying by population estimates from the World Population Prospects 2012 revision[45] and the Human Mortality Database for people older than age 5 years. For the under-5 age groups, we applied the method of Wang and colleagues.[33] In some cases, assumptions in the UN estimation process led to implausible population numbers for some countries and age groups—for example, low population estimates for older age groups in South Africa, especially for the most recent years. For GBD 2013, we applied a Bayesian population reconstruction model[46] to re-estimate population for South Africa for 1970–2013.

Cause of death database

Lozano and colleagues[3] described the key steps in the development of the GBD cause of death database. The database has been expanded to capture 2233 additional site-years of vital registration data and 52 additional verbal autopsy site-years (table 1); a site-year is defined as data for a specific geographical location (eg, a province of China) in a given year. We included data up to April 15, 2014.

	All geographies			GBD 2013		
	GBD 2010	GBD 2013	Difference	National	State, province, or region*	Local
Vital registration	2798	5039	2241†	2765	2112	162
Cancer registry	2715	3860	1145	1216	979	1665
Sibling history	1557	1798	241	1788	0	10
Police records	1129	1433	304	1429	1	3
Surveillance	128	1430	1302	73	1074	283
Verbal autopsy	486	538	52	110	0	428
Survey or census; hospital; burial or mortuary	154	146	−8‡	94	0	52
Total	8967	14244	5277	7475	4166	2603

GBD=Global Burden of Disease Study. *Data were analysed at the state level for Mexico, the province level for China, and the region level for the UK. †Significant increase because of incorporation of subnational sites in China, Mexico, and the UK. ‡Decrease caused by omission of World Health Survey data where adequate vital registration data was available for GBD 2013.

Table 1: **Number of site-years in database by source type**

A major new addition was the incorporation of two data systems in China. First, the China National Office for Maternal and Child Health Surveillance provided detailed information for child and maternal mortality by cause from 363 surveillance sites in China for 1996–2013. Second, the Disease Surveillance Points system was the main source of mortality data for 1991–2007, with 145 disease surveillance points used from 1991 to 2003, and 161 points used from 2004 to 2007. From 2008 to 2012, all of the deaths and cause of death information from the Disease Surveillance Points system and other system points throughout China were collected and reported via the Mortality Registration and Reporting System, an online reporting system of the Chinese Center for Disease Control and Prevention, which included 4·0 million deaths in 2012.[47,48] Because of the discrepancy in proportions of deaths in hospital and out of hospital in the Mortality Registration and Reporting System, we divided each province in China into two strata based on the degree of urbanisation from the 2010 China Census. We then applied the proportion of deaths in hospital and out of hospital and degree of urbanisation from the Disease Surveillance Points system to the Mortality Registration and Reporting System to account for biases in the latter. We disaggregated data for both systems by province and urban and rural regions within each province. We obtained new datasets for Russia that provided more detailed causes (appendix pp 180–244). Turkey expanded its vital registration system to cover nearly all the population after 2009 and we incorporated these new data into the analysis.

In total, we identified 538 verbal autopsy site-years, 52 more than in GBD 2010. India, Bangladesh, and Tanzania had the most verbal autopsy site-years

For the **Human Mortality Database** see http://mortality.org/

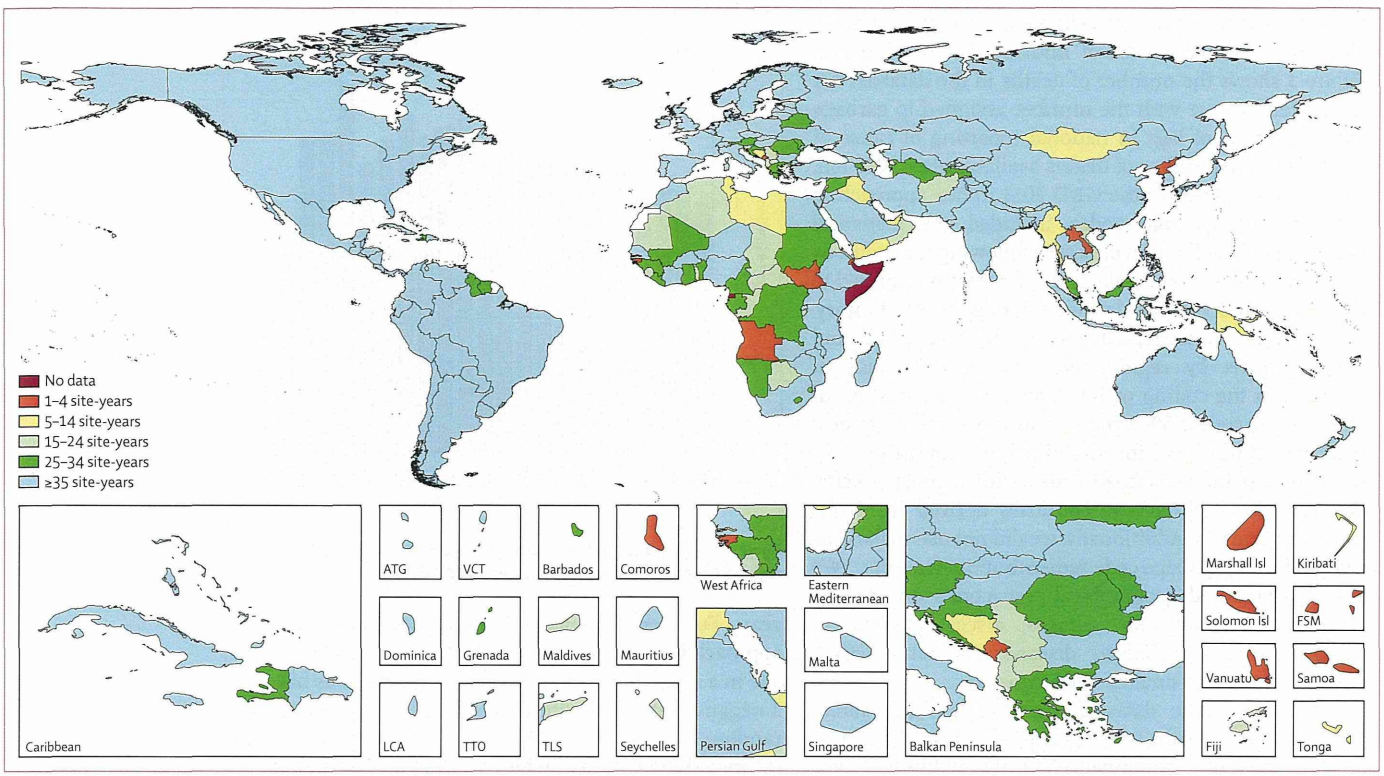

Figure 2: **Site-years for all causes of death data by country, 1980–2013**
ATG=Antigua and Barbuda. VCT=Saint Vincent and the Grenadines. LCA=Saint Lucia. TTO=Trinidad and Tobago. TLS=Timor-Leste. FSM=Federated States of Micronesia.

available. We re-extracted and re-mapped data from all verbal autopsy studies to ensure consistency with the GBD 2013 cause list. We excluded from the database verbal autopsy studies reporting cause assignment using InterVA because it has very low published validity.[47] We incorporated 1145 registry-years of new cancer data, including 128 from Cancer Incidence in Five Continents Volume X[48] and 1017 from supplemental sources. Our analysis of cancer incidence and models of the death:incidence ratio remains unchanged from GBD 2010. Figure 2 shows site-years of data by country for any cause. Of note, Somalia and Equatorial Guinea had no cause of death data for any specific cause.

Assessment and enhancement of quality and comparability of cause of death data

Using the general approach of the GBD 2010, we followed six steps to assess the quality of data and enhance comparability. First, we adjusted cause of death data from vital registration systems for incompleteness. The analysis of all-cause mortality yields a separate estimate of completeness for deaths of children younger than 5 years and deaths of people older than 5 years, which we used to correct the data for cause of death. When correcting for incomplete registration, we assumed that for each age-sex-country group, the cause of death composition of registered deaths and non-registered deaths were the same. 77% of datapoints were from registration or sample registration that were more than 85% complete, 17% from systems that were 70–84% complete, and 6% were from systems less than 70% complete. Of the 6% of observations less than 70% complete, most (62%) were for children younger than 5 years. In sensitivity tests in the GBD 2010, exclusion of data below a fixed threshold of completeness for child causes of death did not substantially change the results; thus, we have used all the data in our analysis for GBD 2013.[3]

Second, we developed 103 maps (excluding verbal autopsy studies) to translate causes found in the data to the GBD 2013 cause list. The expanded cause list of this study required us to adjust the maps used for data included in GBD 2010. Appendix pp 245–251 show GBD 2013 cause maps for International Classification of Diseases 9 and 10. The appendix (pp 252–253) includes more detail about changes made to the handling of various shorter tabulation lists used by some countries for reporting, such as the International Classification of Diseases 9 Basic Tabulation List.

Third, a crucial aspect of enhancing the comparability of data for cause of death is to deal with uninformative, so-called garbage codes. Garbage codes are codes for which deaths are assigned that cannot or should not be considered as the underlying cause of death—for

example, heart failure, ill-defined cancer site, senility, ill-defined external causes of injuries, and septicaemia. Figure 3 shows the number of deaths in the database for each calendar year with the number assigned to garbage codes. Because of lags in national reporting of cause of death data, the number of deaths available after 2010 fell. Important changes for the GBD 2013 in our approach to redistributing garbage codes included the statistical estimation of the fraction of deaths following the methods outlined by Ahern and colleagues[49] for deaths assigned to ill-defined cancer site, ill-defined external causes of injury, heart failure, unspecified stroke, hypertension, and atherosclerosis by region, age, and sex. Because of variation in the coding of International Classification of Diseases 10 code X59 (exposure to unspecified factor)[50] and its subcauses in high-income countries, we redistributed these garbage codes with country-specific estimates for high-income countries derived from our statistical analysis. Additionally, we did not use malaria as a target for any garbage code redistribution in adults.[51] We also implemented geographical restrictions on garbage code redistribution for Chagas disease based on endemicity so that Chagas disease was not assigned deaths in countries outside Latin America.

Fourth, for some datasets, particularly some verbal autopsy studies, deaths were reported for broad age groups or with both sexes combined. With the addition of new data for GBD 2013, we identified 30 new age formats, totalling 112 unique age tabulations in the database. We used the algorithms described in the GBD 2010 to split these aggregated categories into estimates for specific age-sex groups.

Fifth, because few overall deaths were included in verbal autopsy studies or reported in small countries, the number of deaths by cause can fluctuate substantially from year to year. For example, in Iceland, no maternal deaths were recorded from 1991 to 2000, then one maternal death in 2001. We modified our approach to smoothing these stochastic fluctuations used in the GBD 2010 by use of a simple Bayesian algorithm. We assume a normally distributed prior and a normal data likelihood, such that:

$$\text{Posterior mean} = \left(\frac{\tau^2}{\tau^2+\sigma^2}X + \frac{\sigma^2}{\tau^2+\sigma^2}\mu\right)$$

$$\text{Posterior variance} = \left(\frac{\tau^2\sigma^2}{\tau^2+\sigma^2}\right)$$

Where X is the mean of the data and μ is the mean of the prior. We estimated the prior for vital registration series with a negative binomial regression with fixed effects for year and age estimated separately for each country. When the data are based on a large sample size the variance is small and the prior has little effect on the posterior. When the data have a large variance because of a small sample size, the prior has more effect, effectively borrowing strength on the age pattern from data within the same country but allowing for different levels in each year. For verbal autopsy studies, we modified this approach because many published reports are for a single site in a single year. The prior for each cause was based on a negative binomial with fixed effects for age groups and random effects for study-year; the regression was estimated independently for each region. For malaria, we did not group studies by region but by super-region and level of endemicity. To avoid very large negative values for log death rates or logit cause fractions, we limited the minimum non-zero posterior values to 1 per 10 000 000.

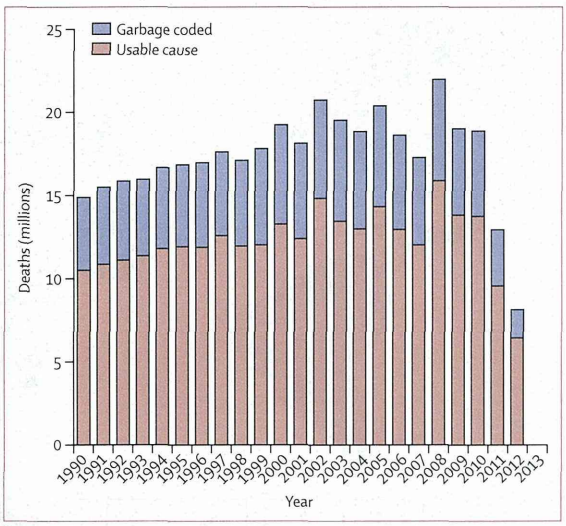

Figure 3: **Total garbage and non-garbage coded deaths from vital registration and verbal autopsy sources, 1990–2013**

Sixth, we excluded outliers based on four criteria. (1) Studies with biologically implausible values, such as 100% of mortality from a single rare cause. (2) Studies with results that were greatly inconsistent with other studies for the same country. (3) Studies that were greatly inconsistent with studies from other countries with similar sociodemographic profiles within the same region. (4) Studies that, if included, led to abrupt changes in model-estimated time trends that could not be explained by contextual changes or policy initiatives. Outliers (0·89% of database entries) are shown in the online data visualisation of the cause of death database.

For **online data visualisation of the cause of death database** see http://vizhub.healthdata.org/cod

Modelling individual causes of death

As in the GBD 2010, we used six modelling strategies for causes of death depending on the strength of the available data. Where extensive data were available, we used cause of death ensemble modelling (CODEm), where fewer data were available we used simpler statistical models, and where available cause of death data might be substantially biased or not available we used natural history models (appendix pp 278–282). We generated 95% UIs from all the modelling strategies. Uncertainty in the number of deaths for an age-sex-country-year was propagated into the computation of years of life lost (YLLs) for the same category.

We used CODEm for 155 causes of death. CODEm has been extensively used for global health estimation including the GBD 2010.[3,52,53] An advantage is that a wide range of different models are tested; only models meeting predetermined criteria for statistical significance and direction of regression coefficients are retained. We excluded 30% of the data from the initial analysis so that the performance of different models could be assessed in terms of how well they predict the omitted data. Through multiple iterations of this process (cross-validation), we obtained stable objective information about the model's performance. The best performing models in terms of root-mean squared error for level and trend were combined into a model ensemble. For some causes, we developed separate ensemble models for GBD developed and GBD developing regions;[54] the main advantage of this approach is that uncertainty in model estimation from heterogeneous data in low-income regions does not inflate the UI for high-income countries. We used this approach for all cancers and transport injuries.

For 13 causes, the number of deaths in the cause of death database was too low to generate stable estimates. For these causes, we developed negative binomial regressions with either a constant or constant multiplied by the mean assumption for the dispersion parameter, using reverse step-wise model building. We selected between the two model dispersion assumptions on the basis of best fit to the data. Compared with the GBD 2010, we modified how we generated uncertainty from these regressions by including in the uncertainty sampling draws from the γ distribution with shape equal to the expected rate (μ) divided by expected dispersion, and scale equal to the expected dispersion if the dispersion was assumed to be constant. For models in which dispersion was assumed to equal a constant multiplied by the mean, the scale parameter included μ as a multiplicative term (instead of the shape parameter).

As in the GBD 2010, for 14 causes for which death is rare, we first modelled the parent cause in the GBD hierarchy with CODEm and then allocated deaths to specific causes using proportions of the parent cause for each sub-cause. For these causes, we identified no significant predictors in negative binomial regressions. We estimated proportions by simple averaging based on available vital registration data. Depending on the availability of data, we averaged the data across age, sex, region, and year.

We used DisMod-MR[55] to estimate detailed cause fractions for several causes of death that had sufficient data to estimate proportions of a parent cause resulting from subcauses that vary across regions and countries but insufficient data to run CODEm. The source code for estimation is available online. DisMod-MR uses data for subcause fractions gathered from systematic review and from International Classification of Diseases-coded vital registration and sample registration systems. It uses two types of fixed effects (study characteristics and country covariates) with hierarchical random effects for super-region, region, and country to generate estimates for each country, age group, both sexes, and six discrete time points: 1990, 1995, 2000, 2005, 2010, and 2013. We calculated predictions for intervening years—and back to 1980—assuming an exponential rate of change. We used this approach for eight causes of maternal death, four causes of meningitis, one cause of chronic kidney disease, four causes of cirrhosis, four causes of liver cancer, and three causes of haemoglobinopathies.

For 14 causes in the GBD 2010, we used natural history models because data systems for cause of death did not capture sufficient information. The natural history model for African trypanosomiasis was updated to include the most recent case notification data from WHO (up to 2012). We made substantial changes to the HIV natural history model.[25] Our natural history model for congenital syphilis was estimated as in the GBD 2010, with updated data for antenatal care coverage to inform the number of births at risk and additional vital registration data sources to inform age and sex distribution of deaths. We also used simple natural history models for typhoid and paratyphoid fever, whooping cough, measles, visceral leishmaniasis, and yellow fever. Additionally, because vital registration data recording the specific type of hepatitis were very sparse, we used natural history models for all the detailed causes of hepatitis. The natural history model takes into account the extensive serological data for the prevalence of antibodies or antigens for hepatitis A, B, and C, and more limited data for case-fatality rates.

Alzheimer's disease and other dementias were analysed with CODEm in GBD 2010. Because of the large inconsistency between the data for prevalence and mortality, we used a natural history model in the GBD 2013. Prevalences have not changed substantially over time, whereas age-standardised mortality rates in high-income countries have increased, ranging from about 25% (Denmark, Switzerland, Norway) to 46% (Germany). The prevalence of dementia varies between countries by a factor of three, whereas dementia mortality recorded in vital registration data and verbal autopsy studies varies by more than 20-fold. On the basis of these findings, we believe that the variation in dementia mortality rates between countries and over time was probably affected by changes in coding practices with increased propensity to assign dementia as an underlying cause of death. To correct for this, we assessed data from 23 high-income countries with high-quality vital registration systems to estimate the ratio of registered dementia deaths:prevalent cases. In DisMod-MR, we used the mean of these ratios as an estimate of excess mortality to estimate age-specific and sex-specific mortality from dementia consistent with the meta-regression of prevalence.

In GBD 2010, because single-cause models were developed for each cause, the final step was to combine

For the **source code for estimation** see http://ghdx.healthdata.org/node/156633

these models into estimates that are consistent with all-cause mortality for each age-sex-country-year group. For each cause-specific model and for all-cause mortality, we had 1000 draws from the posterior distribution for each age-sex-country-year group. We combined causes by taking a random draw without replacement from the posterior distribution of each cause and all-cause mortality. Each cause was rescaled by a scalar equal to the draw of all-cause mortality divided by the sum of the draws of individual causes. The GBD 2010 induced a correlation of 1·0 between the sum of cause-specific and all-cause mortality. CoDCorrect was applied in a hierarchical fashion: first to level 1 causes and then to level 2 and level 3 causes. Level 2 causes were constrained to sum to the level 1 parent cause. Levels of this cascade were largely the same as those used in the GBD 2010 and were chosen on the basis of the amount and quality of available data for cause of death.

For GBD 2013, we made slight modifications to this approach. Because tests showed no substantial effect of the 1·0 correlation between draws of all-cause mortality and the sum of individual causes and because each cause is modelled independently such that the ordering of draws across causes were unrelated, we have removed this assumption. Furthermore, because the modelling of HIV through the GBD version of Spectrum uses relationships between incidence, CD4 progression, and death that are age-dependent and antiretroviral therapy scale-up over time has had major effects, we modified the way in which HIV deaths are handled in CoDCorrect. We ran CoDCorrect for all causes and then computed the pre-CoDCorrect cumulative deaths over time and age and compared with the cumulative deaths post-CoDCorrect. This provided an overall scalar, which we used to adjust the entire HIV epidemic. To avoid in any age-sex-country-year the sum of individual deaths exceeding all-cause mortality, we computed the difference between the cumulatively scaled HIV deaths and the CoDCorrect HIV deaths and added this difference to the estimate of all-cause mortality at the draw level.

In GBD 2010, diarrhoea deaths and lower respiratory infection deaths were reported for pathogen-specific causes in tabulations that summed to 100% of each parent cause. Since the GBD 2010, the GEMS study[56] has been published, which provided data for the relative risk of diarrhoea being related to different pathogens. This relative risk approach used a different conceptual framework than did the International Classification of Diseases approach for underlying cause. Underlying cause follows the more than 200-year history of health statistics of assigning each death uniquely to a single underlying cause. The relative risk approach follows the approach used more generally for risk factors, where cause is assigned based on comparison to a counterfactual. Counterfactual attribution to specific risks or in this case pathogens, can sum to more or less than 100%. On the basis of the GEMS study and consultations among experts in both diarrhoea and lower respiratory infection, we report results for counterfactual causes in GBD 2013. To estimate diarrhoea mortality attributable to different pathogens, we calculated the population attributable fraction for pathogens including rotavirus, *Shigella*, enteropathogenic *Escherichia coli*, enterotoxigenic *E coli*, adenovirus (enteric adenovirus), norovirus, *Aeromonas*, other *Salmonella* (non-typhoidal *Salmonella*), *Cryptosporidium*, *Campylobacter*, and *Entamoeba*. We used the Miettinen formula, which uses the distribution of pathogens in patients and relative risks of pathogens for diarrhoea, to provide a population attributable fraction for each pathogen:[57,58]

$$PAF_i = p_i(pathogen\ in\ patients)\left(1 - \frac{1}{odds\ ratio_i}\right)$$

Where PAF_i is the population attributable fraction of diarrhoea caused by pathogen i, p_i is the prevalence of pathogen i in patients with diarrhoea, and $odds\ ratio_i$ is the odds ratio of diarrhoea in people with the pathogen. We used DisMod-MR to estimate the proportion of patients in each age-sex-country-year with each pathogen with data from studies of inpatients and community samples. By use of study-level covariates in the meta-regression, we obtained different estimates for inpatients and community samples. We assumed inpatients to be a proxy for severe diarrhoea and death. We reanalysed GEMS[59] to estimate the odds ratio for each pathogen in a multipathogen model by conditional logistic regression. Regression models included fixed effects for a specific pathogen with interaction terms for three age groups (0–1 years, 1–2 years, and 2–6 years) to allow different odds ratios by age and interaction terms for different GEMS field sites (Bangladesh, India, Kenya, Mali, Mozambique, Pakistan, and The Gambia) to estimate site-specific odds ratios. For other countries in the region, the odds ratio we used was the average of the odds ratios (in logarithm scale) of the countries with GEMS sites in that region. For countries in central and southern sub-Saharan Africa, we used the average of GEMS sites located in eastern and western sub-Saharan Africa. For all other countries in regions without GEMS sites, we used the average of all odds ratio. To produce odds ratio uncertainty while averaging odds ratio, we generated 1000 draws of joint normal distribution using a covariance matrix from the conditional logistic regression for each of the GEMS countries in a region. To produce the draws for non-GEMS countries, we selected draws from each of the GEMS countries until we had a full set of 1000 draws. For example, to generate 1000 draws for countries in eastern sub-Saharan Africa, we used draws from Kenya and Mozambique—the two GEMS countries within that region. We pulled 500 of the Kenya draws and 500 of the Mozambique draws to produce our full set of

1000 draws, which were used for all the other countries in this region. Because GEMS included only diarrhoea in children younger than 5 years, we applied the odds ratio of pathogens calculated for children aged 2–5 years when calculating for adults. We did not assign diarrhoea cases or deaths to a pathogen for an age-country-year if more than 95% of draws were greater than 1.

For cholera, we used data from previous studies (appendix p 310) and compared them with WHO case notification data to estimate under-reporting for cholera and then the number of cases (appendix p 310). To estimate cholera deaths, we modelled cholera case fatality in DisMod-MR with data from previous studies.

Clostridium difficile as a cause of diarrhoea in children is rarely studied; we could not estimate the epidemiological population attributable fraction as we did for other pathogens because *C difficile* was not included in GEMS. Because *C difficile* is related to hospital and health-care use, we used hospital data as the primary source for estimation. We modelled the incidence and case fatality of *C difficile* and assumed a 1-month risk of death[60] in DisMod-MR to estimate the number of deaths.

For GBD 2013, we split lower respiratory infection mortality into four categories: *Streptococcus pneumoniae*, *Haemophilus influenzae* type B pneumonia, respiratory syncytial virus pneumonia, and influenza. The counterfactual approach captures the complex interactions between the these causes[61] and also excludes the "other lower respiratory infection" category included in GBD 2010. Moreover, we did not attribute lower respiratory infection to any cause for children younger than age 1 month. We adopted a different approach to estimate bacterial and viral causes on the basis of available data. For pneumococcal and *H influenzae* type B pneumonia, we estimated the causal fraction from vaccine efficacy studies.[62–64] For pneumococcal pneumonia, we included data from controlled trials and observational studies, such as before-after population analyses of the introduction of pneumococcal vaccine.[65–76] For *H influenzae* type B, we excluded case-control studies because of implausibly large estimates of vaccine efficacy. Furthermore, unlike for pneumococcal vaccine, little data were available from vaccine efficacy studies on the effect outside of child ages. As a result, we did not estimate the causal fraction of *H influenzae* type B for lower respiratory infection in people aged 5 years or older. We adjusted data for efficacy, using invasive disease as a marker as well as serotype coverage for pneumococcal vaccine.[64] We calculated pooled estimates of causal fractions by age with DisMod-MR for pneumococcal vaccine and random-effects meta-analysis for *H influenzae* type B, adjusted post-hoc for national-level coverage of pneumococcal vaccine and *H influenzae* type B vaccine. For respiratory syncytial virus and influenza, we relied on observational studies that measured causal fractions among hospital admissions for lower respiratory infection. We estimated the causal fractions among cases by country, age, and sex with DisMod-MR and the odds ratio of exposure from case-control studies. To account for the higher case-fatality of bacterial versus viral lower respiratory infections, we applied a relative case-fatality differential based on in-hospital case-fatality using hospital admissions that included cases coded to the specific pneumonia causes.

Convergence measures

To test whether all-cause and cause-specific mortality converged in the 188 countries since 1990, we computed two measures: the average relative difference and the average absolute difference between any pair of countries included in the GBD 2013 study. The average relative difference is known as the Gini coefficient and is the most commonly used measure of inequality. For international comparisons, we used the population-weighted version of the Gini coefficient in age-specific mortality rates so that small populations do not have an undue influence on the assessment of global mortality convergence (appendix pp 556–557).[77] For the Gini coefficient to fall, the percent decrease in mortality for countries with higher mortality must in general be faster than that for countries with lower mortality.

We also computed the mean absolute difference for all-cause mortality for each age group for 1990–2013 and for age-standardised rates for each cause (appendix pp 556–557). Average absolute difference can fall while average relative difference (the Gini coefficient) rises. The two measures provide different perspectives on convergence.

Multiple decrement lifetables

We used age-specific cause of death and all-cause mortality life-tables to compute the conditional probability of death for three summary intervals: childhood and adolescence (0 to exact age 15 years), reproductive-age adults (15 years to exact age 50 years), middle-aged adults (50 years to exact age 75 years), and the cause-specific contributions to each of these summary indicators. For each conditional probability of death, we used the multiple decrement life-table method[78] to compute the probability of death from each cause and the overall contribution of each cause of death to the summary probability of death indicators for the three broad age groups (appendix pp 556–557). We calculated the decomposition of changes in life expectancy by age and cause of death as detailed by Beltran-Sanchez, Preston, and Canudas-Romo.[79]

Age-standardised rates and YLLs

For GBD 2010, we computed age-standardised mortality rates and YLL rates from the world population age standard issued by WHO in 2001.[80] To account for the substantial change in global demographics since 2001, we updated this standard. We used the same method as

WHO and computed a standard population structure with population estimates for 2010–35 from the most recent World Population Prospects by the United Nations Population Division. Appendix pp 95–96 provides details of the GBD world population age-standard. We computed YLLs by multiplying numbers of deaths from each cause in each age group by the reference life expectancy at the average age of death for those who die in the age group following the standard GBD 2010 methods.[3] The appendix (pp 121–40) shows key indicators from the new GBD standard life-table.

Ranking lists and decomposition analysis

We used the GBD 2010 approach to create ranked lists of specific diseases and injuries. We modified GBD 2010 ranking list to incorporate newly estimated causes with the same overall assignment of rank causes as GBD 2010: typhoid and paratyphoid separately, haemolytic disease in fetus and newborn and other neonatal jaundice, mesothelioma, unintentional suffocation, pulmonary aspiration and foreign body in trachea or lung, and foreign body in other part of body. Following the methods developed by Lozano and colleagues,[3] we decomposed changes in the number of global deaths and global YLLs into the contributions from population growth, population aging, and age-specific death rates.

Role of the funding source

The funder of the study had no role in study design, data collection, data analysis, data interpretation, or writing of the report. The authors had access to the data in the study and the final responsibility to submit the paper.

Results

Global all-cause mortality

Global life expectancy at birth for both sexes increased from 65·3 years in 1990, to 71·5 years in 2013, an average increase of 0·27 years per calendar year. Life expectancy increased over this period by 6·6 years for females and 5·8 years for males. Figure 4 shows the yearly change in global life expectancy at birth, with a large drop in the 1990s as a result of the Rwanda genocide and famine in North Korea and the return to increases of about 0·3 years or more per year since 2003. If the median rate of change of the last 23 years continues, by 2030 global female life expectancy will be 85·3 years and male life expectancy will be 78·1 years. Reduced fertility and the consequent demographic shift of the world's population to older ages has led to the mean age of death increasing from 46·7 years in 1990, to 59·3 years in 2013.[81]

The number of deaths globally for both sexes all ages increased from 47·47 (UI 46·77–48·22) million in 1990, to 54·86 (53·57–56·33) million in 2013, partly because of consistent increases in global population over the past

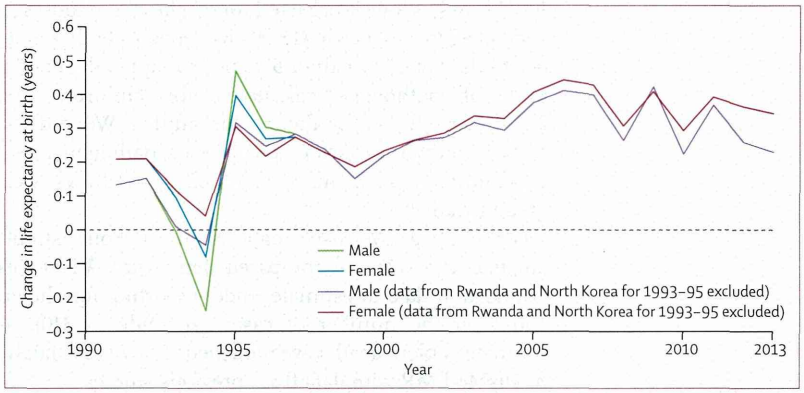

Figure 4: **Change in global life expectancy at birth for males and females**

decades. Rapid falls in child death rates compared with other age-specific death rates have led to a shift in the age structure of global deaths with substantial decreases in children and large increases in the proportion of deaths of people older than age 80 years (figure 5). The number of child deaths fell between 1990 and 2013 in southeast Asia, east Asia, and Oceania with very substantial falls in north Africa and the Middle East, and Latin America and the Caribbean (figure 5). However, the number of child deaths in sub-Saharan Africa only changed from 3·68 (3·63–3·73) million in 1990, to 3·20 (3·00–3·42) million in 2013. Substantial increases in the number of deaths of people older than age 80 years have occurred in high-income regions as well as in southeast Asia, east Asia, and Oceania.

Rising global life expectancy at birth has not come from uniform progress across age-groups or countries. In all age-groups except the 80 years and older age group, mean mortality rate has decreased more for females than for males (figure 6). Larger decreases in males older than age 80 years might be a result of the differences in the age composition between males and females in this open-ended age group. The mortality rate in the under-5 age group has fallen much more between 1990 and 2013 than has that for older age groups. The smallest decreases occurred in men in age groups 30–34 years, 35–39 years, and 80 years or older, and in women aged 80 years or older.

For all age groups, population-weighted average relative difference for age-specific mortality rates differences across countries (ie, inequality) increased except in age group 10–14 years and 15–19 years for females. The divergence in age-specific mortality rates was greatest in young adult age groups between ages 20 years and 44 years for both males and females; dominant causes in these age groups include HIV/AIDS, interpersonal violence, maternal mortality, and road injury (data not shown). For many age groups, in both sexes, the absolute differences have fallen while relative inequalities have increased (figure 6). For women aged 25–39 years and 75 years and older, and for men aged 20–49 years and 65 years and

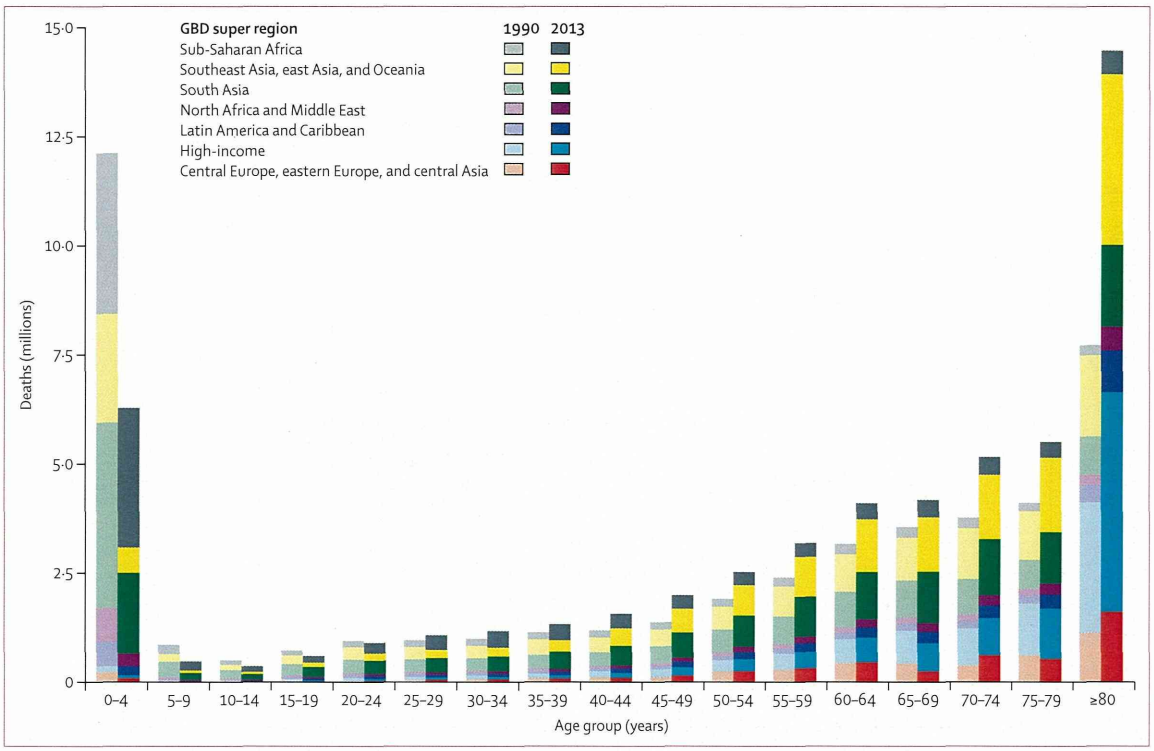

Figure 5: **Global deaths by age and super region in 1990 and 2013**

older, both relative and absolute differences in mean age-specific mortality rates have increased since 1990.

Global causes of death

We decomposed change in global and regional life expectancy by cause (level 2 of the GBD cause hierarchy; figure 7). Increased life expectancy since 1990 was mainly caused by a fall in mortality from lower respiratory infections and diarrhoeal diseases (contributing 2·2 years), cardiovascular and circulatory diseases (contributing 1·1 years), neonatal conditions (contributing 0·7 years), cancers (contributing 0·4 years), and chronic respiratory diseases (contributing 0·5 years). Decreases in mortality from unintentional injuries added another 0·3 years to life expectancy, while female life expectancy increased by about 0·2 years because of reductions in maternal mortality. These gains were offset by increased mortality from diabetes, chronic kidney diseases, and related conditions, as well as musculoskeletal disorders, although the net effect of these increases was small, reducing life expectancy, on average, by about 0·1 years. Five main causes reduced life expectancy: HIV/AIDS was a major cause of death in southern sub-Saharan Africa and to a smaller extent in western and eastern sub-Saharan Africa; diabetes, chronic kidney disease, and other endocrine disorders decreased life expectancy across many regions, most notably in Oceania and central Latin America; mental disorders made a negative contribution in multiple regions, especially high-income north America; intentional injuries reduced life expectancy in south Asia, high-income Asia Pacific, and southern sub-Saharan Africa; and cirrhosis made a negative impact in eastern Europe and central Asia (figure 7). Large gains in life expectancy in sub-Saharan Africa were mainly driven by reductions of diarrhoea and lower respiratory infections and of neonatal disorders. Gains in high-income regions were driven by reductions in cardiovascular disease, some cancers, transport injuries, and chronic respiratory conditions (figure 7).

Between 1990 and 2013, numbers of deaths from non-communicable diseases and injuries steadily increased while deaths from communicable, maternal, neonatal, and nutritional causes decreased (table 2). However, age-standardised rates decreased in these three broad categories. The shift to non-communicable diseases, at least at globally, was driven by faster rates of decline for communicable, maternal, neonatal and nutritional causes and an ageing world population.

In 2013, 11·8 million (11·3–12·3) deaths were caused by communicable, maternal, neonatal, and nutritional disorders: 2·7 million (2·4–2·8) by lower respiratory infections, 1·3 million (1·3–1·5) by HIV/AIDS, 1·3 million (1·2–1·4) by tuberculosis, and 1·3 million (1·2–1·4) by diarrhoeal diseases, 2·0 million (1·9–2·2) by neonatal conditions, 854 600 (702 924–1 032 497) by malaria, and 293 336 (261 322–328 200) by maternal causes (about 20%